On the Existence of a Fully Developed Wind-Sea Spectrum

G. J. KOMEN,[1] S. HASSELMANN, AND K. HASSELMANN

Max-Planck-Institut für Meteorologie, Hamburg, FRG

(Manuscript received 17 January 1984, in final form 29 May 1984)

ABSTRACT

We consider the energy transfer equation for well-developed ocean waves under the influence of wind, and study the conditions for the existence of an equilibrium solution in which wind input, wave–wave interaction and dissipation balance each other. For the wind input we take the parameterization proposed by Snyder and others, which was based on their measurements in the Bight of Abaco and which agrees with Miles's theory. The wave–wave interaction is computed with an algorithm given recently by S. Hasselmann and others. The dissipation is less well-known, but we will make the general assumption that it is quasi-linear in the wave spectrum with a factor coefficient depending only on frequency and integral spectral parameters. In the first part of this paper we investigate whether the assumption that the equilibrium spectrum exists and is given by the Pierson–Moskowitz spectrum with a standard type of angular distribution leads to a reasonable dissipation function. We find that this is not the case. Even if one balances the total rate of change for each frequency (which is possible), a strong angular imbalance remains. Thus the assumed source terms are not consistent with this type of asymptotic spectrum. In the second part of the paper we choose a different approach. We assume that the dissipation is given and perform numerical experiments simulating fetch-limited growth, to see under which conditions a stationary solution can be reached. For the dissipation we take K. Hasselmann's form with two unknown parameters. From our analysis it follows that for a certain range of values of these parameters, a quasi-equilibrium solution results. We estimate the relation between dissipation parameters and asymptotic growth rates. For equilibrium spectra, the input, dissipation and nonlinear-transfer source functions are all significant in the energy-containing range of the spectrum. The energy balance proposed by Zakharov and Filonenko in 1966 and Kitaigorodskii in 1983, in which dissipation is assumed to be significant only at high frequencies, yields a spectrum that grows too rapidly and does not approach equilibrium. One of our equilibrium solutions has a one-dimensional spectrum that lies close to the Pierson–Moskowitz spectrum. However, the angular distribution differs in some important features from standard spreading functions. The energy balance of this equilibrium spectrum is analyzed in detail.

1. Introduction

The problem of evolution of ocean waves under the influence of wind has been the subject of many studies. It is known that the spectral wave-energy density changes in space and time as the result of several different physical processes: the propagation of energy, the energy input by wind forcing, the dissipation of energy through wave breaking (white-capping) or turbulence, and the exchange of energy between different wave components interacting weakly among themselves. In practice, all these processes compete, their relative importance varying with the wind-field history and the coastal geometry.

To simplify the problem we will consider the case of fetch-limited wave growth in deep water and with a constant wind field. For this situation many observations have led to a fairly detailed understanding of wind-sea evolution. In particular, it was found (Hasselmann *et al.*, 1973) that the shape of the spectrum remains approximately similar, so that the evolution of the wind sea can be summarized by growth curves of relatively few characteristic parameters.

Mathematically, the evolution of waves is described by the energy transfer equation (Hasselmann, 1960; Willebrand, 1975). In this equation the various physical processes are represented by source terms. It is evident that there must be a close relationship between the properties of these source terms and the observed spectral evolution. In fact, qualitatively many of the observed features of wave growth can be understood in terms of known properties of the source terms: the peak frequency decreases with fetch because the nonlinear interactions transfer energy to lower frequencies; the growth rate decreases when the dominant wave speed approaches the wind speed, because energy transfer from the atmosphere is reduced; the high-frequency part of the spectrum has a nearly fetch-independent shape, because in that range the source terms balance. However, despite our general understanding of observed wave growth and the quantitative support of these concepts by computations of various source functions for individual spectra, explicit nu-

[1] On leave of absence from Royal Netherlands Meteorological Institute, De Bilt, The Netherlands.

merical simulations of fetch-limited wave growth in wave models have not been entirely satisfactory. For instance, spectral models describing wave evolution normally make *ad hoc* assumptions about the way in which an asymptotic stage is reached and use parameterizations of the nonlinear interactions in this region that are not based on exact calculations, but are constructed to reproduce the desired growth characteristics (SWAMP, 1984).

A basic problem with numerical wave-growth simulations has been the difficulty of obtaining reliable estimates of the nonlinear transfer, since straightforward integration of the relevant Boltzmann integrals requires excessive computing time. However, in recent years several improved integration routines have been written (Webb, 1978; Masuda, 1980; Hasselmann *et al.,* 1984a) and the one used by us was fast enough to allow a series of numerical wave-growth experiments to be made. An earlier account is given by Hasselmann and Hasselmann (1984).

From this work it became clear that the detailed evolution of the wave spectrum is a rather subtle problem. This is related to the large number of degrees of freedom in a spectral description and the fact that all three source functions (input, dissipation and nonlinear transfer) contribute significantly to the energy balance in the main region of the spectrum. The resulting energy balance is basically of a two-scale structure. On a small spatial (or fast temporal) scale the three source functions achieve an approximate balance through the rapid adjustment of the spectral shape. The remaining small imbalance then determines the actual evolution of the spectrum on a larger (slower) scale. Although the general features of the spectral shape and the migration of the spectrum towards lower frequencies are largely controlled by the nonlinear transfer (cf. Hasselmann *et al.,* 1973), one finds that the details of the spectrum near the peak and thereby also the quantitative growth rates also depend sensitively on the form of the input and dissipation source functions.

Fetch-limited wave growth may be divided into three stages: an early stage, with a power-law evolution of the parameters, a transitional stage, and a late stage with strongly reduced growth. Because of the complexity of the full problem we will limit our attention in the present paper to the final stage. The initial and transitional stage will be discussed in a second paper (Hasselmann *et al.,* 1984b). The application of the results of these studies for numerical wave models using a parameterized form of the nonlinear transfer is considered by Hasselmann *et al.* (1984a).

It is useful to study the final stage first as this eliminates some of the uncertainties in the dissipation source function. The dissipation level may be expected to depend on the mean wave steepness, but it is not known in which manner. The growth rates and the transition from the early to the final growth stage are quite sensitive to the way this wave-steepness dependence is chosen. In the discussion of the energy balance of a fully developed spectrum, however, the wave-steepness dependence does not appear explicitly, but can be simply absorbed in the general empirical constant of the dissipation source function.

The paper consists of three parts. In Section 2 we summarize what is known today about the source terms, in Section 3 we study the energy balance for the conventional Pierson–Moskowitz spectrum as candidate of a quasi-equilibrium solution, and in Section 4 we present the results of our numerical experiments.

2. The energy transfer equation

The evolution of ocean wave spectra can be described by the energy transfer equation (Hasselmann, 1960; Willebrand, 1975), which for deep water in the absence of currents takes the form

$$\frac{\partial F}{\partial t} + \mathbf{c}_g \nabla F = S_{\mathrm{in}} + S_{\mathrm{nl}} + S_{\mathrm{dis}}, \qquad (2.1)$$

where $F = F(\mathbf{k}; \mathbf{x}, t)$ is the two-dimensional wave spectrum, which varies with $\mathbf{x}$, t on space-time scales large compared to a typical wave length or period. Wave energy propagates with the group velocity $\mathbf{c}_g$ and is changed by the three source terms on the right-hand side representing the wind input, nonlinear wave–wave interactions and dissipation.

For the wind input we take the parameterization proposed by Snyder *et al.* (1981) on the basis of direct measurements of the work done by the atmospheric pressure fluctuations on the waves,

$$S_{\mathrm{in}}(\mathbf{k}) = \max\left[0,\, 0.25\, \frac{\rho_a}{\rho_w}\left(\frac{u_5}{c_p}\cos\theta - 1\right)\omega F(\mathbf{k})\right]. \qquad (2.2)$$

Here ρ_a and ρ_w represent the densities of air and water, $\omega = 2\pi f$, u_5 is the wind speed at 5 m, c_p is the phase velocity of waves with frequency f, and θ is the angle between the wind vector and the wave propagation direction. The measurements were made in the range $1 < (u_5/c_p)\cos\theta < 3$. More recent measurements by D. E. Hasselmann, *et al.* (1984) at larger fetches in the North Sea, which provided more data particularly near $u_5/c_p \approx 1$, are consistent with (2.2). Eq. (2.2) has to be modified for $u_5/c_p > 3$ (cf. Plant, 1982; Mitsuyasu and Honda, 1982) but we will not need this extension for our present work. In its range of validity, Eq. (2.2) is in reasonable agreement with the theory of Miles (1959), provided it is suitably redefined in terms of u_*/c_p, where the friction velocity $u_* = (\tau_a/\rho_a)^{1/2}$ is determined by the wind shear stress τ_a.

The importance of scaling wave growth with u_* rather than with the wind speed at a fixed height has been stressed by many workers (Miles, 1959; Pierson, 1964; Mitsuyasu and Honda, 1982; Plant, 1982; Janssen and Komen, 1984). Nevertheless, wave growth analysis has often been carried out in terms of the wind speed at a fixed height, for lack of wind-stress data. If the ratio between u_* and u_5 were constant, this would be immaterial. However, there is ample evidence that the ratio increases with wind speed (cf. Smith and Banke, 1975; Smith, 1980). From general dimensional considerations, Charnock (1955) derived a universal relation for the increase of the drag coefficient $C_z = u_*^2/u_z^2$ with the wind speed u_z at height z in the constant stress layer. Wu (1982) recently showed that Charnock's relation can be well approximated by the simpler formula

$$C_{10} = u_*^2/u_{10}^2 = (0.8 + 0.065u_{10}) \times 10^{-3}, \quad (2.3)$$

which is consistent with many observations over a large range of wind speeds. According to (2.3), the u_*/u_{10} ratio varies by as much as a factor of $\sqrt{2}$ if u_{10} varies from 5 to 25 m s^{-1}. This clearly has important consequences for wave modelling. If e.g. the dimensionless wave energy $E_* = Eg^2/u_*^4$ for a fully developed spectrum, expressed in terms of u_*, were a universal constant (which could be argued on dimensional grounds) then the dimensionless maximum wave energy expressed in terms of u_{10} would vary over this wind speed range by a factor of 4. As important as this scaling question is, it is still far from resolved, as illustrated by the SWAMP (1984) study. Most of the models compared in the study scaled with u_{10}, but several models were also based on u_*-scaling. All models were tuned against measurements and were claimed to give satisfactory predictions.

We shall adopt u_*-scaling, following the dimensional arguments of Charnock (1955), Kitaigorodskii (1962) and others: if u_* is the only external parameter defining the structure of the atmospheric boundary layer and its coupling to the ocean, and the generating mechanism is linear, the input source function must be of the form $S_{\rm in} = B(u_*/c_p)\, F(\mathbf{k})$, independent of the detailed form of the assumed wave-generating mechanism. We shall accordingly express Eq. (2.2) in terms of u_*, taking $u_5 \approx 0.94u_{10}$, and $C_{10} = 1.12 \times 10^{-3}$. This value of C_{10} is typical for the values measured directly by Snyder *et al.* (1981) and also follows from Eq. (2.3) for $u_{10} = 5$ m s^{-1}, a typical wind speed for their measurements. With these values we obtain $u_5/c_p \approx 28u_*/c_p$. However, in view of the uncertainties that enter in the derivation of this relation we have chosen a slight generalization, namely $u_5/c_p = 28\beta u_*/c_p$, where β is an empirical factor we expect to be approximately equal to one. In this way we obtain

$$S_{\rm in}(\mathbf{k}) = \max\left[0,\, 0.25\,\frac{\rho_a}{\rho_w} \times (28\beta(u_*/c_p)\cos\theta - 1)\omega F(\mathbf{k})\right]. \quad (2.4)$$

The range of uncertainty of β is indicated by Mitsuyasu and Honda (1982), who scaled the Snyder *et al.* parameterization using $u_5 = 23u_*$, which is equivalent to $\beta \approx 0.85$. The effect of small variations of β on the spectral energy balance will be discussed in Sections 3 and 4.

The second source function $S_{\rm nl}$ describes the nonlinear energy transfer due to resonant third-order wave–wave interactions and is given by the Boltzmann-integral expression (Hasselmann, 1961)

$$S_{\rm nl}(\mathbf{k}) = \omega \int d\mathbf{k}_1 d\mathbf{k}_2 d\mathbf{k}_3 \sigma(\mathbf{k}_1, \mathbf{k}_2, \mathbf{k}_3, \mathbf{k}) \times \hat{\delta}\,(\mathbf{k}_1 + \mathbf{k}_2 - \mathbf{k}_3 - \mathbf{k})\delta(\omega_1 + \omega_2 - \omega_3 - \omega) \times [n_1 n_2(n_3 + n) - n_3 n(n_1 + n_2)], \quad (2.5)$$

where the action density $n(\mathbf{k}) = F(\mathbf{k})/\omega$, $\omega = (gk)^{1/2}$ and $n_i = n(\mathbf{k}_i)$.

The integral kernel σ represents a net scattering coefficient proportional to the square of an interaction coefficient (Hasselmann, 1963a). Equation (2.5) has been integrated numerically by several workers, using standard integration techniques (Hasselmann, 1963b; Cartwright, 1966, unpublished; Sell and Hasselmann, 1972; Webb, 1978; Masuda, 1980). The δ-functions were eliminated by projection onto the three-dimensional resonance subspace of the six-dimensional $\mathbf{k}_1 \cdot \mathbf{k}_2 \cdot \mathbf{k}_3$, space. Integrable singularities which arise along the caustics of the resonance surfaces are normally removed by using stretched coordinates.

Because of the extensive computing time required in the past to evaluate (2.5), various approximations to the exact expression have also been considered. Narrow-peak expansions (Longuet-Higgins, 1976; Fox, 1976; Dungey and Hui, 1979) reproduce many of the qualitative features of the exact expressions, but are nevertheless not sufficiently good approximations for typical wind-sea spectra to be applied in detailed quantitative investigations of the spectral energy balance. Similar limitations apply for the dispersion-operator approximation for small scattering angles (Hasselmann and Hasselmann, 1981; Hasselmann *et al.*, 1984a). An accurate and fast algorithm for the computation of (2.5) remains an important requirement for systematic studies of the nonlinear transfer.

In this paper we use a new integration technique which makes use of the symmetry properties of the integrand by introducing symmetric variables at the outset (Hasselmann and Hasselmann, 1981, and Hasselmann *et al.*, 1984a), thereby reducing the computing time considerably. Further saving is achieved by precomputing the integration grid and the interaction coefficient, and filtering out unimportant regions of phase space. A compilation of results obtained with this method for a variety of spectra is given by Hasselmann and Hasselmann (1981).

For the dissipation source term $S_{\rm dis}$ we follow Hasselmann (1974). Under rather general conditions, the dissipation was shown to be quasi-linear in the wave spectrum, with a coefficient ψ_d which depends only on the wavenumber and integral spectral parameters, such as the average wave steepness,

$$S_{\rm dis}(\mathbf{k}) = -\psi_d(\mathbf{k})F(\mathbf{k}). \tag{2.6}$$

For whitecapping processes that are short in duration and spatial scale compared with the characteristic periods and wavelengths of the spectrum, Hasselmann found $\psi_d \sim k$. The complete evaluation of $\psi_d(\mathbf{k})$ is an outstanding problem in ocean-wave research. It is a complicated problem requiring both a detailed knowledge of the hydrodynamics of breaking waves and the translation of the analysis of individual breaking events into a spectral description.

In Section 3 we describe a first attempt to infer $\psi_d(\mathbf{k})$ for a fully developed spectrum from the requirement that for this situation the dissipation should just balance the wind input and nonlinear transfer. However, this approach is not very fruitful, as the conclusions are found to be very sensitive to the assumed spectral distribution. In fact, the standard Pierson–Moskowitz spectrum and angular spreading functions yield unrealistic dissipation functions.

In Section 4 we adopt therefore the alternative approach of exploring the consequences of specifying a particular parameterization for $\psi_d(\mathbf{k})$. We assume the general form

$$S_{\rm dis}(\mathbf{k}) = -c\bar{\omega}\left(\frac{\omega}{\bar{\omega}}\right)^n\left(\frac{\hat{\alpha}}{\hat{\alpha}_{\rm PM}}\right)^m F(\mathbf{k}) \tag{2.7}$$

in agreement with Hasselmann (1974) (for $n = 2$) and Hasselmann and Hasselmann (1984). Here $\hat{\alpha}$ is the integral wave-steepness parameter

$$\hat{\alpha} = E\bar{\omega}^4/g^2,$$

where

$$\bar{\omega} = E^{-1}\int F(\mathbf{k})\omega d\mathbf{k}$$

and $\hat{\alpha}_{\rm PM} = 4.57 \times 10^{-3}$ is the theoretical value of $\hat{\alpha}$ for a Pierson–Moskowitz spectrum [Eq. (3.1)]. For a Pierson–Moskowitz spectrum (or generally for a JONSWAP type spectrum with fixed shape parameters) $\hat{\alpha}$ is proportional to Phillips' constant α.

The constants c and n in (2.7) determine the overall level of dissipation and the position of the maximum dissipation relative to the peak of the frequency spectrum, respectively. We shall treat them as adjustable tuning parameters. The power m determines the dependence of dissipation on wave steepness. As pointed out above, this parameter is important for growing wind seas (cf. Hasselmann *et al.*, 1984b), but is irrelevant for the present investigation, since for a quasi-fully-developed spectrum choosing different values of m is equivalent to redefining c. We have taken $m = 2$ in all of our computations.

3. Energy balance of the Pierson–Moskowitz spectrum

From the analysis of a set of well developed wind-sea spectra obtained with a shipborne wave recorder in the North Atlantic, Pierson and Moskowitz (1964) proposed the form

$$F_{\rm PM}(f) = \frac{\alpha g^2}{(2\pi)^4 f^5}\exp\left[-\frac{5}{4}\left(\frac{f_{\rm PM}}{f}\right)^4\right] \tag{3.1}$$

for the frequency spectrum of a fully developed wind sea, where Phillips' constant $\alpha = 0.0081$, and the peak frequency $f_{\rm PM}$ is related to the wind speed at 19.5 m by

$$f_{\rm PM} = 0.14g/u_{19.5} \tag{3.2}$$

In terms of 10 m winds u_{10}, Eq. (3.2) may be written

$$f_{\rm PM} = 0.13g/u_{10}. \tag{3.3}$$

The selection of fully developed spectra was based on the synoptic situation. It was ensured that no swell was present and that the fetch and duration were sufficiently large to expect a stationary and homogeneous fully developed wave state (Moskowitz, 1964). However, there is no strict experimental evidence that the Pierson–Moskowitz spectrum really corresponds to a stationary state in a constant wind field, since infinite fetch and infinite duration do not occur in nature, and even for very large fetch and duration, there may always be a small residual growth which escapes detection. Exceptionally stationary wind conditions can be found in tropical wind systems, but even these exhibit significant fluctuations. In a wave hindcast study for the South China Sea, for example, Chang *et al.* (1983) found that disturbances originating in midlatitudes can lead to an occasional doubling of the wind speed of the monsoon in that area. Similarly, in wave measurements east of Barbados, Regier and Davis (1977) found important spectral contributions at frequencies below the Pierson–Moskowitz frequency, which were ascribed to remote wind intensification. At all events, however, it seems plausible that the growth rates for well developed waves are strongly reduced, and in fact most wave models take the Pierson–Moskowitz spectrum or a variation thereof as a stationary limiting spectrum. It is of interest therefore to test whether the spectral form (3.1) is consistent with a stationary solution of the energy transfer equation and our knowledge of the source terms summarized in the previous section.

To investigate this question we need to rewrite (3.3) first in terms of u_*. This was stressed already by Pierson and Moskowitz (1964), and indeed the arguments of the previous section in favour of u_*-scaling for $S_{\rm in}$ apply equally here. Again the question arises as to the appropriate drag coefficient to use for the conversion. Since the observations of Moskowitz

(1964) were made for wind speeds between 10 and 20 m s^{-1}, we should choose a drag coefficient corresponding to this wind-speed range. We have taken the mean SWAMP value $C_{10} = 1.8 \times 10^{-3}$, which corresponds to a wind speed $u_{10} = 15$ m s^{-1} for the drag law (2.3). Thus we set

$$f^*_{\rm PM} = f_{\rm PM} u_*/g = 5.6\ 10^{-3}, \qquad (3.4)$$

$$E^*_{\rm PM} = E_{\rm PM} g^2/u_*^4 = 1.1\ 10^3. \qquad (3.5)$$

[The Pierson–Moskowitz energy $E_{\rm PM} = 0.2\alpha g^2 \times (2\pi f_{\rm PM})^{-4}$ follows from integration of (3.1).]

To study the full two-dimensional energy balance we need to make also an assumption about the angular distribution of the wave spectrum. Many wave models assume a simple $\cos^2\theta$ distribution about the wind direction. The experimental evidence, however, suggests that the angular distribution is frequency dependent and narrower near the peak frequency f_m. On the basis of their own measurements and a summary of earlier work, Hasselmann *et al.* (1980) suggest the following directional distribution for a growing wind sea

$$F(f, \theta) = F(f)D(f, \theta)$$

where the spreading factor

$$D(f, \theta) = N_p^{-1} \cos^{2p}(\theta/2) \qquad (3.6)$$

with

$$p = 9.77(f/f_m)^\mu, \qquad (3.7)$$

$$\mu = \begin{cases} 4.06, & f < f_m \\ -2.34, & f > f_m. \end{cases}$$

The normalization constant

$$N_p = 2^{1-2p}\pi \frac{\Gamma(2p+1)}{\Gamma^2(p+1)}$$

is defined such that $\int_{-\pi}^{+\pi} D d\theta = 1$.

In this section we assume the angular distribution (3.6) throughout. However, we also performed all calculations with a simple $\cos^2\theta$ distribution, with similar results.

Figure 1 shows $S_{\rm in}(f)$ and $S_{\rm nl}(f)$ (integrated over θ) as computed for the Pierson–Moskowitz spectrum (3.1), (3.3), and (3.6). The wind input is given by (2.4) with $\beta = 0.85$ in accordance with Mitsuyasu and Honda (1982). If the Pierson–Moskowitz spectrum is in equilibrium, the sum of $S_{\rm in}$ and $S_{\rm nl}$ must be balanced by the dissipation,

$$\text{“}S_{\rm dis}\text{”} = -S_{\rm in} - S_{\rm nl}.$$

The dissipation “$S_{\rm dis}$” inferred by this relation is also shown in Fig. 1. It has positive values at about 1.4 times the peak frequency. If we require the dissipation to be negative, it follows that our assumptions cannot be consistent. One could argue that the discrepancy is not serious because the range over which positive values occur is rather small. But even if $S_{\rm dis}$ were zero in this range the dissipation would still contain two highly implausible pronounced minima. The origin of these problems is easily recognized. The inferred positive values of “$S_{\rm dis}$” result from the

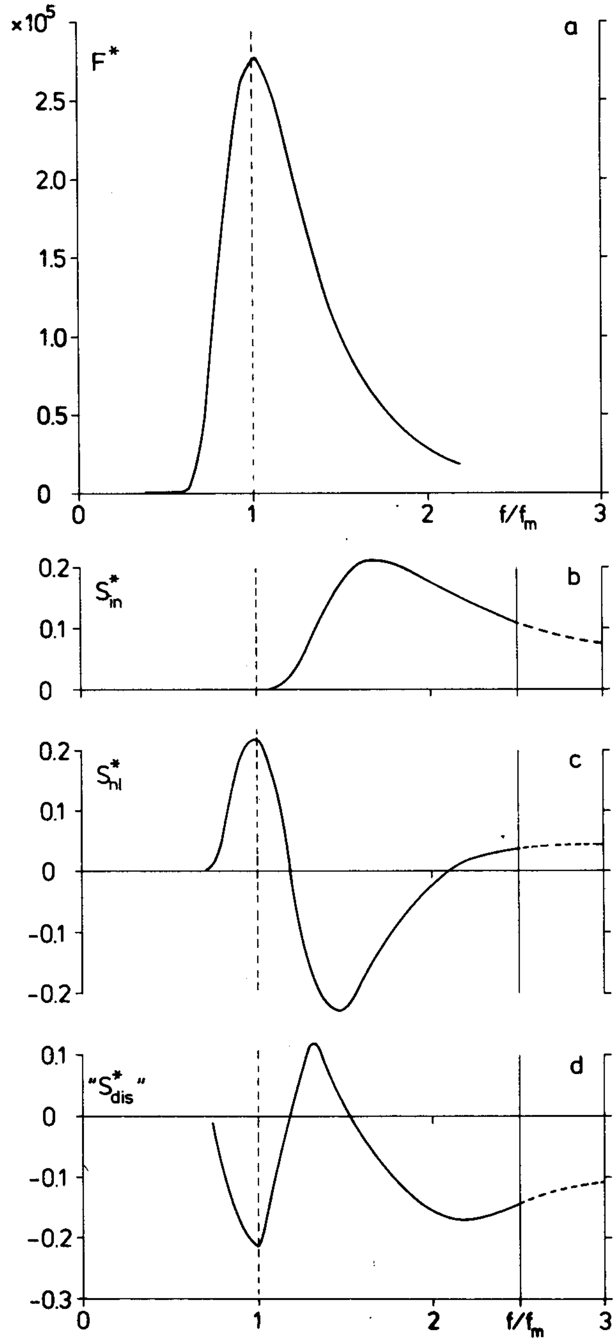

FIG. 1. Source terms for Pierson–Moskowitz spectrum (3.1) with spreading function (3.6). The input source function (panel b) is given by Eq. (2.4) with $\beta = 0.85$. The dissipation source function “$S^*_{\rm dis}$” is computed as a residual from $S^*_{\rm in} + S^*_{\rm nl} +$ “$S^*_{\rm dis}$” $= 0$. All functions are nondimensionalized in terms of g and u_*.

gap between the positive low-frequency lobe of the nonlinear transfer and the wind input maximum. In addition, the nonlinear transfer appears rather too large and is driving the dissipation to adopt a similar, but inverted distribution.

On the basis of these observations it may be anticipated that the nature of the balance is quite sensitive to the precise values of α and β. A reduction of α reduces the relative importance of the nonlinear transfer, which scales with α^3, while the spectrum and thus S_{in} scale with α. An increase in β tends to close the gap between the spectral peak and wind input maximum. To demonstrate this explicitly, Fig. 2 shows the results of computations analogous to Fig. 1, but with $\alpha = 0.005$ and $\beta = 1.02$. The one-dimensional dissipation is seen now to be an acceptable function of frequency, and one could be tempted to conclude that the Pierson–Moskowitz spectrum, with $\alpha = 0.005$, represents a conceivable stationary solution of the energy balance equation.

However, the picture is less satisfactory if we turn now to the directional distributions. Fig. 3 shows the two-dimensional transfer function (15° intervals) corresponding to the case shown in Fig. 2. The two-dimensional dissipation has been calculated from (2.6) assuming

$$\psi_d(f) = S_{\text{dis}}(f)/F(f) \tag{3.8}$$

with $S_{\text{dis}}(f)$ given as in Fig. 2 (i.e., the factor ψ_d is assumed to be isotropic, and we have ensured that the directionally integrated net rate of spectral change at any frequency vanishes). The figure indicates a strong angular imbalance, which must lead to a redistribution of energy. Thus our tentative equilibrium spectrum is in fact clearly not a stationary solution of the transfer equation. This was confirmed by numerical integrations in which we simulated the wave evolution starting from a Pierson–Moskowitz spectrum with $\alpha = 0.005$ and $\beta = 1.02$. The spectrum rapidly changed to a new spectrum with a new angular distribution, for which the source terms were then no longer balanced even for the one-dimensional frequency distributions.

This may have been anticipated also on the basis of Webb's (1978) calculations, in which he showed that for the Pierson–Moskowitz spectrum the nonlinear energy transfer is directed away from the mean direction. A transfer of this form cannot be balanced with the directional dependencies assumed for our input and dissipation source functions. We conclude that the Pierson–Moskowitz spectrum with the spreading function (3.6) cannot represent a stationary solution of the energy transfer equation for the form of source functions assumed in Section 2.

To continue, we could attempt to construct a balance between all three source functions by appropriate modification of the input and dissipation source functions. However, inspection of the structure of the energy balance suggests that this cannot be successfully achieved using plausible source functions for the assumed spectral distribution (3.1)–(3.6). Therefore, in the next section, we invert the problem and determine the possible asymptotic spectra that may develop from given source functions. This appears a more fruitful approach in view of the sensitivity of the energy balance to small changes in the form of the spectrum. We shall discover that quasi-equilibrium solutions to the energy balance equation do in fact

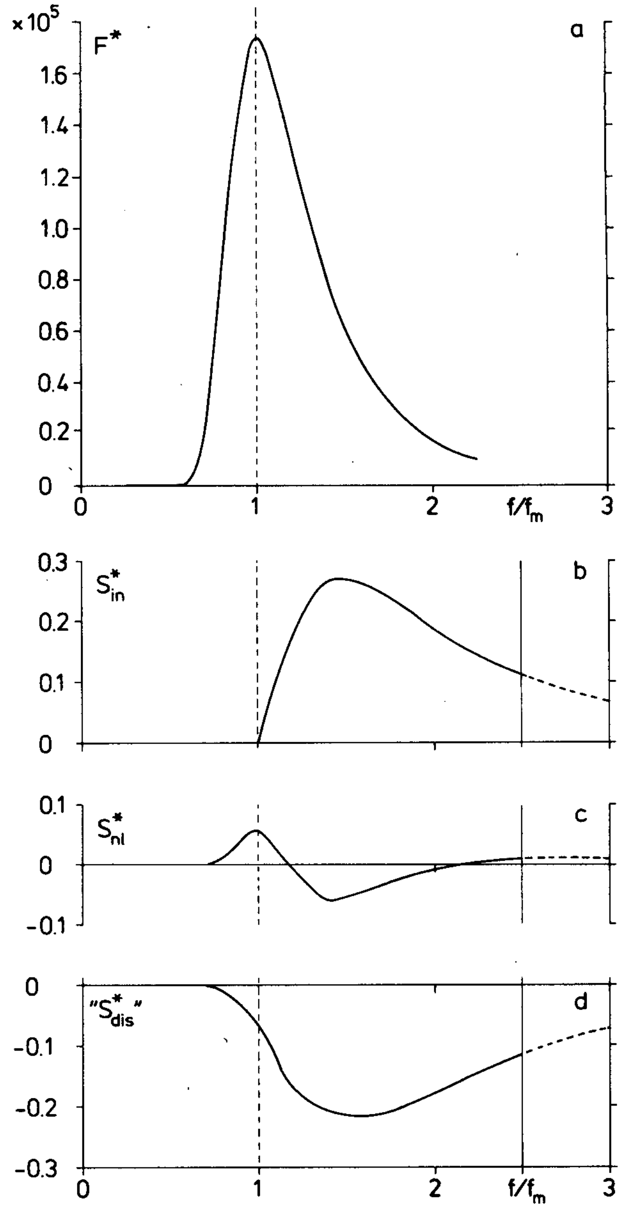

FIG. 2. Source terms for Pierson–Moskowitz spectrum with Phillips' constant changed from 0.0081 to 0.005. The input source function is given by Eq. (2.4) with $\beta = 1.02$. The inferred dissipation source function "S^*_{dis}" (panel d) is computed as a residual from $S^*_{\text{in}} + S^*_{\text{nl}} + $"$S^*_{\text{dis}}$" $= 0$.

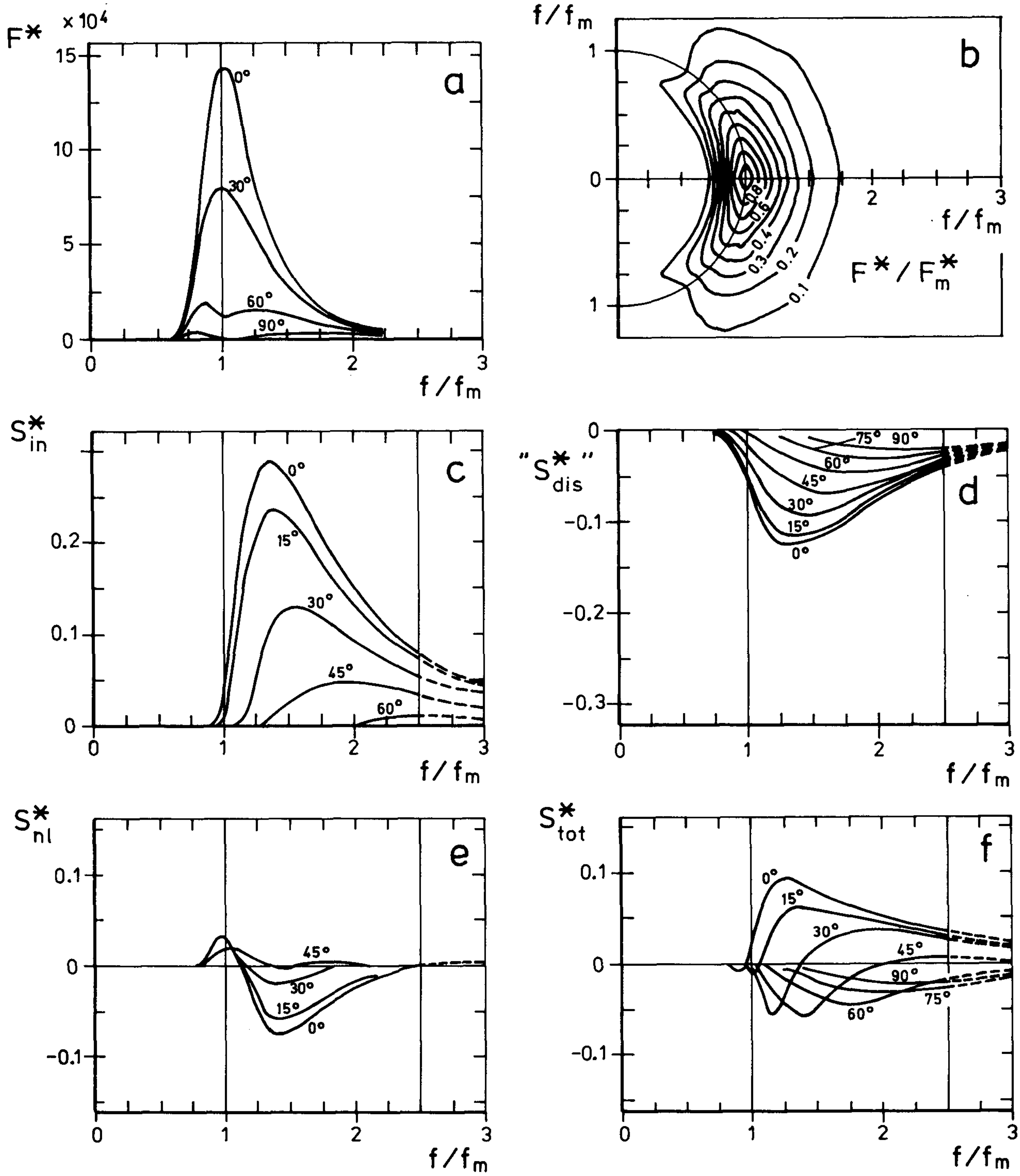

FIG. 3. Two-dimensional spectrum (panel a, with polar isoline representation in panel b) and source functions corresponding to Fig. 2. The two-dimensional dissipation source function "S^*_{dis}" is computed from the one-dimensional distribution of Fig. 2 assuming a directional-independent factor ψ_d in (2.6). The net source function $S^*_{tot} = S^*_{in} + S^*_{nl} +$ "S^*_{dis}" is significantly different from zero.

exist that exhibit frequency spectra rather close to the Pierson–Moskowitz spectrum, but that the directional distributions differ from (3.6) in some minor, yet dynamically essential, features.

4. Simulation of asymptotic wave evolution

The type of numerical growth-simulation experiments discussed in this section are described briefly by Hasselmann and Hasselmann (1984). The transport equation (2.1) is solved numerically for the case $\partial F/\partial t = 0$, taking $F(x = 0) = 0$ as upwind boundary condition. We shall be concerned here particularly with the influence of the dissipation parameters on the solution for large fetches. We used a straightforward first-order forward-difference scheme with a dynamically adjusted Δx. The computations were made with a logarithmic frequency discretization ($f_n = 1.1 f_{n-1}, f_0 = 0.01$) and with an angular resolution of 30°. The spectrum was predicted explicitly in the energy-containing frequency range of $0 < f < 2.5 f_m$. For higher frequencies a Phillips type f^{-5} tail was added. A simple first-order integration scheme was considered adequate, since Δx was determined by the rapidly responding high-frequency region of the spectrum just below the $2.5 f_m$ limit. As a result the ΔF were very small in the energetically relevant region near the spectral peak. A number of runs was made to establish that the results were insensitive to the details of the high-frequency parameterization, the choice of frequency and directional discretization and the numerical integration scheme.

A total of 19 full integration runs, listed in Table 1, was carried out for various combinations of dissipation parameters c and n [cf. Eq. (2.7)]. The wind input term was taken as in (2.4) with $\beta = 1.0$ (different β-values correspond simply to rescaling with different wind speeds). The principal properties of the asymptotic spectra for large fetch are summarized in Fig. 4, which show the distribution of the principal spectral parameters E (total energy), f_m (peak frequency), α (Phillips constant, defined for the frequency range $1.5 f_m < f < 2.5 f_m$) and γ (peak enhancement factor = ratio of spectral value at peak frequency to value of the Pierson–Moskowitz spectrum at this frequency for the same α) in the $c - n$ plane for a fetch of $x^* = 1.2 \times 10^8$. At this fetch most wave models predict an equilibrium spectrum, and the parameters are accordingly normalized by the corresponding values for a Pierson–Moskowitz spectrum. However, only the bottom-right segments of the $c - n$ parameter planes in Fig. 4 actually correspond to equilibrium spectra; in the top-left regions the spectra are still evolving. The associated non-dimensional growth rates

$$\tilde{S}_{\text{tot}} = \frac{1}{\bar{f}} \frac{\bar{c}_g}{E} \frac{\partial E}{\partial X} \tag{4.1}$$

for the total energy at the fetch $x^* = 1.2 \times 10^8$ are shown in Fig. 5, while Figs. 6 and 7 show the growth and growth rates of E as a function of fetch for some sample cases.

With the exception of the zero-dissipation case 00, the growth rates for all spectra are strongly reduced at large fetch. Runs number M2 and H4 yield similar, small asymptotic growth rates and may be regarded as quasi-stationary, but some of the other cases with lower dissipation coefficients c (L2) or higher powers n (M4) still show growth rates that are 4 or 5 times as large at $x^* = 10^8$. Generally, we find no asymptotic growth for high dissipation (high c) and low n, and increasing asymptotic growth for decreasing c and increasing n. It is not difficult to understand this result. A stationary solution can exist only if there is no significant leakage of energy to low frequencies. This is possible only if the low frequency lobe of the nonlinear transfer is balanced by a sufficiently strong dissipation at low frequencies. This requires a sufficiently large value of c. The power n should also not be too large, as this tends to shift the dissipation away from lower to higher frequencies.

The case 00 with no explicit dissipation is seen to be quite unrealistic and yields a continually growing wave spectrum, at a growth rate that far exceeds observed growth rates for fetch-limited waves. It should be noted that the zero-dissipation case 00 corresponds in fact to an energy balance with zero dissipation only in the region below the cut-off frequency $2.5 f_m$. The condition that an f^{-5} frequency tail is maintained for frequencies beyond this cut-off implies an effective dissipation above the cutoff in order to balance the wind input and the nonlinear transfer into this region of the spectrum. Thus case 00 corresponds to the energy balance considered by Zakharov and Filonenko (1966) and Kitaigorodskii (1983), in which there is zero dissipation in the energy-containing range of the spectrum and a sink

TABLE 1. List of runs, with values of spectral parameters and growth rates at large fetch ($x^* = 1.2 \times 10^8$). The letters L, M, MH and H of a run designation refer to the coefficients c = 1.67 (low), 3.33 (medium), 5.00 (medium–high), and 6.67 (high) ($\times 10^{-5}$), respectively, in the dissipation expression (2.7). The index 2, 3 or 4 following the letter(s) refers to the power of ω in (2.7).

Run	$\frac{f_m}{f_{PM}}$	$\frac{E}{E_{PM}}$	$\alpha \times 10^3$	γ	$\left[\frac{c_g}{\bar{f}E}\frac{dE}{dx}\right]_{x^*=1.2\times 10^8}$
L1	1.1	0.87	13.	1.1	10^{-6}
L2	0.92	1.28	9.6	1.3	0.4×10^{-6}
L3	0.91	1.5	7.8	1.6	1.1×10^{-6}
M1	1.44	0.41	15.0	1.2	0.1×10^{-6}
M2	1.0	0.98	9.6	1.0	0.1×10^{-6}
M3	0.97	1.02	8.3	1.1	0.2×10^{-6}
M4	0.82	1.41	5.0	1.6	1.1×10^{-6}
M5	0.84	1.28	4.8	1.9	0.5×10^{-6}
MH1	1.7	0.21	17.0	1.1	0.2×10^{-7}
MH2	1.25	0.49	12.0	1.0	0.5×10^{-7}
MH3	1.07	0.76	8.7	1.0	~0
MH4	0.93	0.96	5.8	1.4	0.3×10^{-6}
MH5	0.86	1.05	4.8	1.5	0.5×10^{-6}
H1	2.0	0.11	19.6	1.1	~0
H2	1.3	0.4	11.0	1.2	~0
H3	1.07	0.64	7.9	1.1	~0
H4	0.95	0.86	5.8	1.1	0.3×10^{-6}
HH2	1.44	0.31	11.0	1.1	~0
00	zero dissipation: strong growth, no equilibrium				

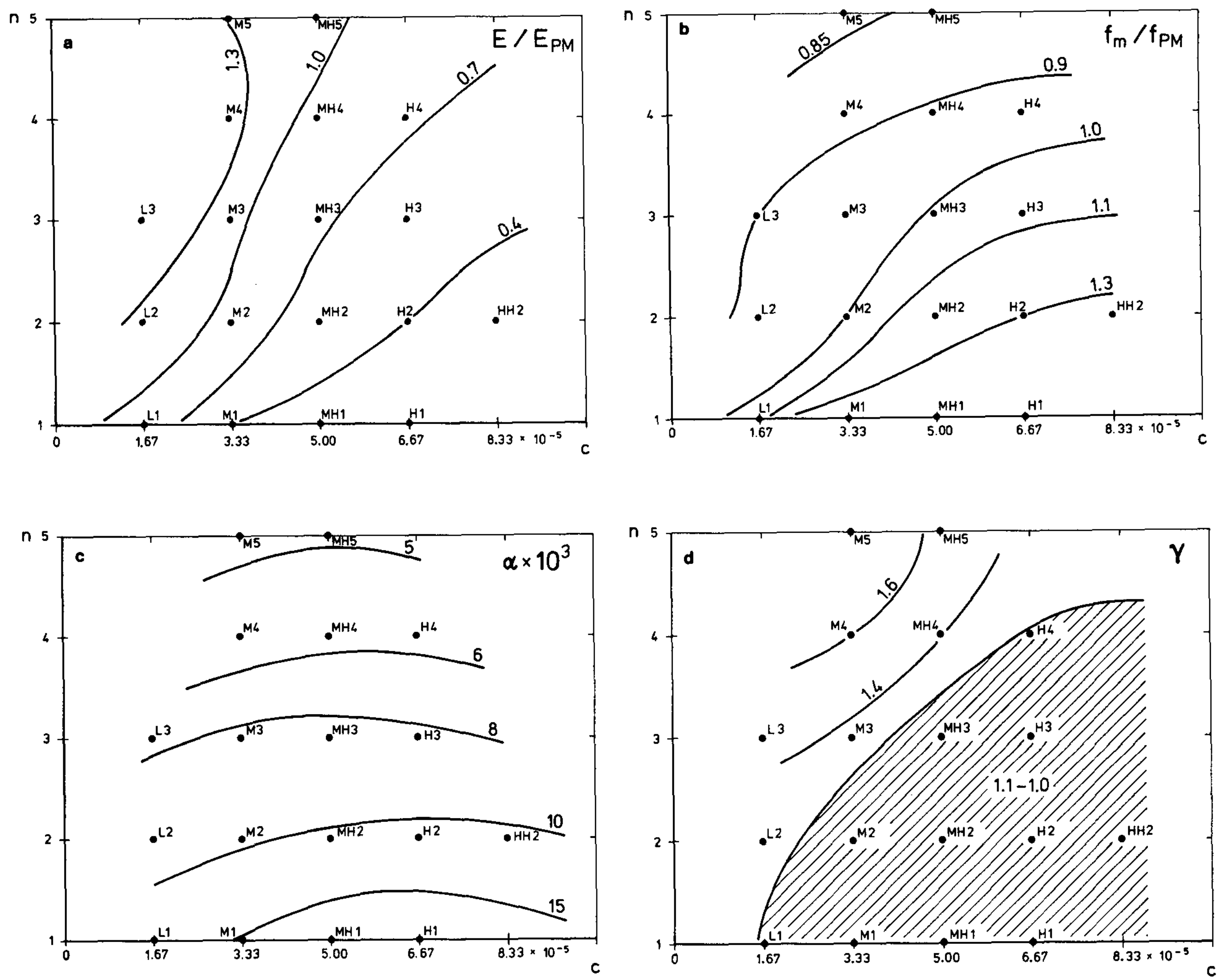

FIG. 4. Distribution of spectral parameters E/E_{PM} (panel a), f_m/f_{PM} (panel b), α (panel c), and γ (panel d) for runs listed in Table 1 in the $c - n$ dissipation parameter plane [cf. (2.7)]. All values are taken at a fetch of $x^* = gx/u^2 = 1.2 \times 10^8$. Isolines are approximate and meant to guide the eye. The best agreement with observations is given by run M2.

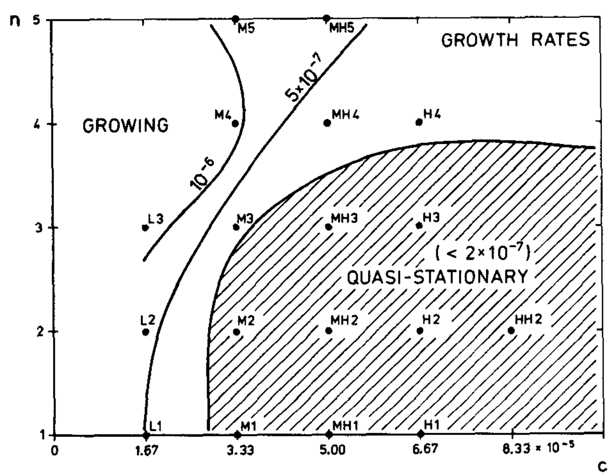

FIG. 5. Asymptotic growth rates $\dfrac{c_g}{fE}\dfrac{dE}{dx}$ at $x^* = 1.2 \times 10^8$.

at high frequencies. Our numerical experiments do not support this form of energy balance.

We have made an attempt to select a best run from our set of 19. Figures 4 and 5 indicate some characteristic trends in the dependencies of the spectral parameters and growth rates on the dissipation parameters c and n. As one moves horizontally to the right of the diagonal separating the stationary from the nonstationary regime (Fig. 5) towards higher coefficients c, the total energy E decreases below the Pierson–Moskowitz value. This is accompanied by a weak increase in the peak frequency and a weak decrease in Phillips' constant α and the peak enhancement factor γ, all of which contribute to the net reduction of E. On the other hand, if one moves upwards and to the right in the direction of the diagonal separating the growth and quasi-stationary regimes, the total energy remains more or less constant, while both α and f_m decrease. The increase in

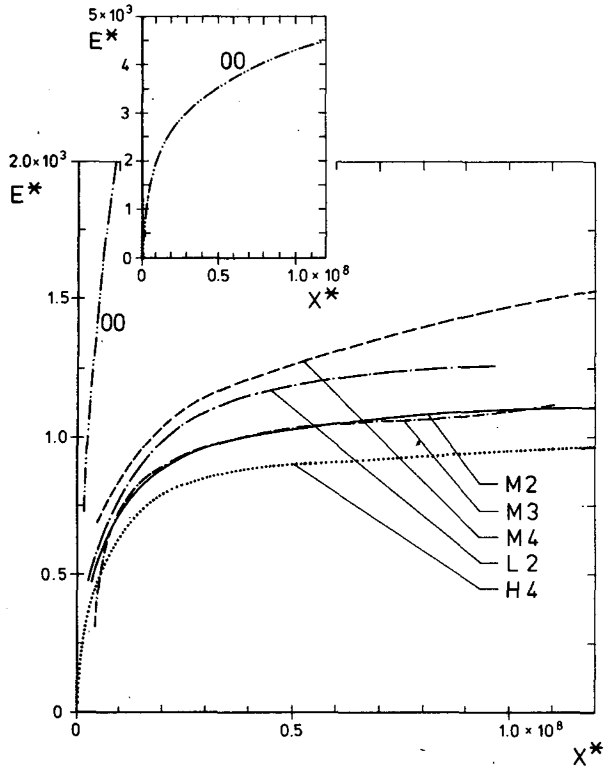

FIG. 6. Energy–fetch growth curves for selected runs of Table 1. Run M2 approaches a quasi-stationary asymptotic state close to the Pierson–Moskowitz spectrum (cf. Fig. 8). Lower coefficients c and higher powers n in the dissipation expression yield spectra which continue to grow at large fetch. Higher coefficients c yield equilibrium sea states with too low energies.

c along the diagonal tends to reduce the total energy, but is counteracted by the increase in n, which shifts the dissipation towards higher frequencies and allows more energy to build up at low frequencies (while reducing the energy level at higher frequencies). Thus although the total energy along the diagonal remains at the Pierson–Moskowitz value, the spectral shape becomes distorted relative to the Pierson–Moskowitz form towards lower frequencies. The best agreement with the Pierson–Moskowitz spectrum is found near the bottom of the diagonal in the neighborhood of run M2 (medium dissipation coefficient, frequency exponent 2). The dissipation for this run is given by

$$S_{\rm dis} = -3.33 \times 10^{-5}(\omega/\bar{\omega})^2 \cdot \bar{\omega}(\hat{\alpha}/\hat{\alpha}_{\rm PM})^2 \cdot F(\mathbf{k}). \quad (4.2)$$

The value of the frequency exponent agrees with Hasselmann's (1974) result for small-scale whitecapping.

Figure 8 shows the evolution of the characteristic spectral parameters E, f_m, α and γ for run M2. The agreement with the Pierson–Moskowitz values for large fetch is excellent (other runs could be adjusted to yield the correct asymptotic energy by varying β, however, a simultaneous agreement of all spectral parameters could be achieved only for this case).

The recovery of an equilibrium spectrum close to the Pierson–Moskowitz form may appear surprising in the light of the discussion of the previous section, in which we found that the Pierson–Moskowitz spec-

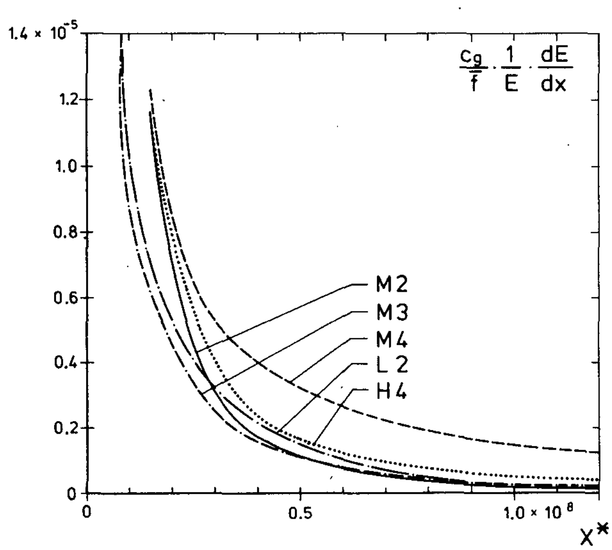

FIG. 7. Nondimensional growth rates corresponding to Fig. 6.

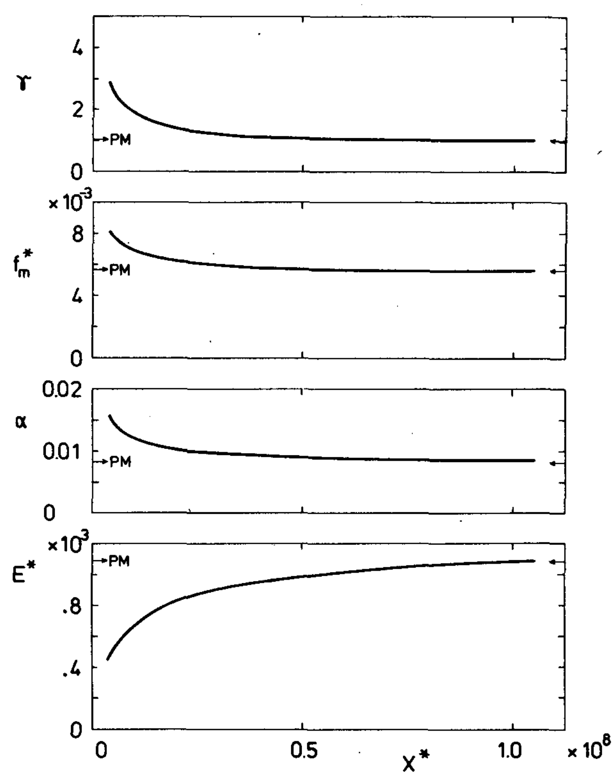

FIG. 8. Growth of spectral parameters for optimal model M2. The Pierson–Moskowitz values are denoted by arrows.

trum with a standard type of angular distribution could not be a stationary solution of the energy transfer equation. The essential difference between our present finding and the conclusion of Section 3 is resolved if we look in detail at the angular properties of the energy balance. Fig. 9, panels a and b, show

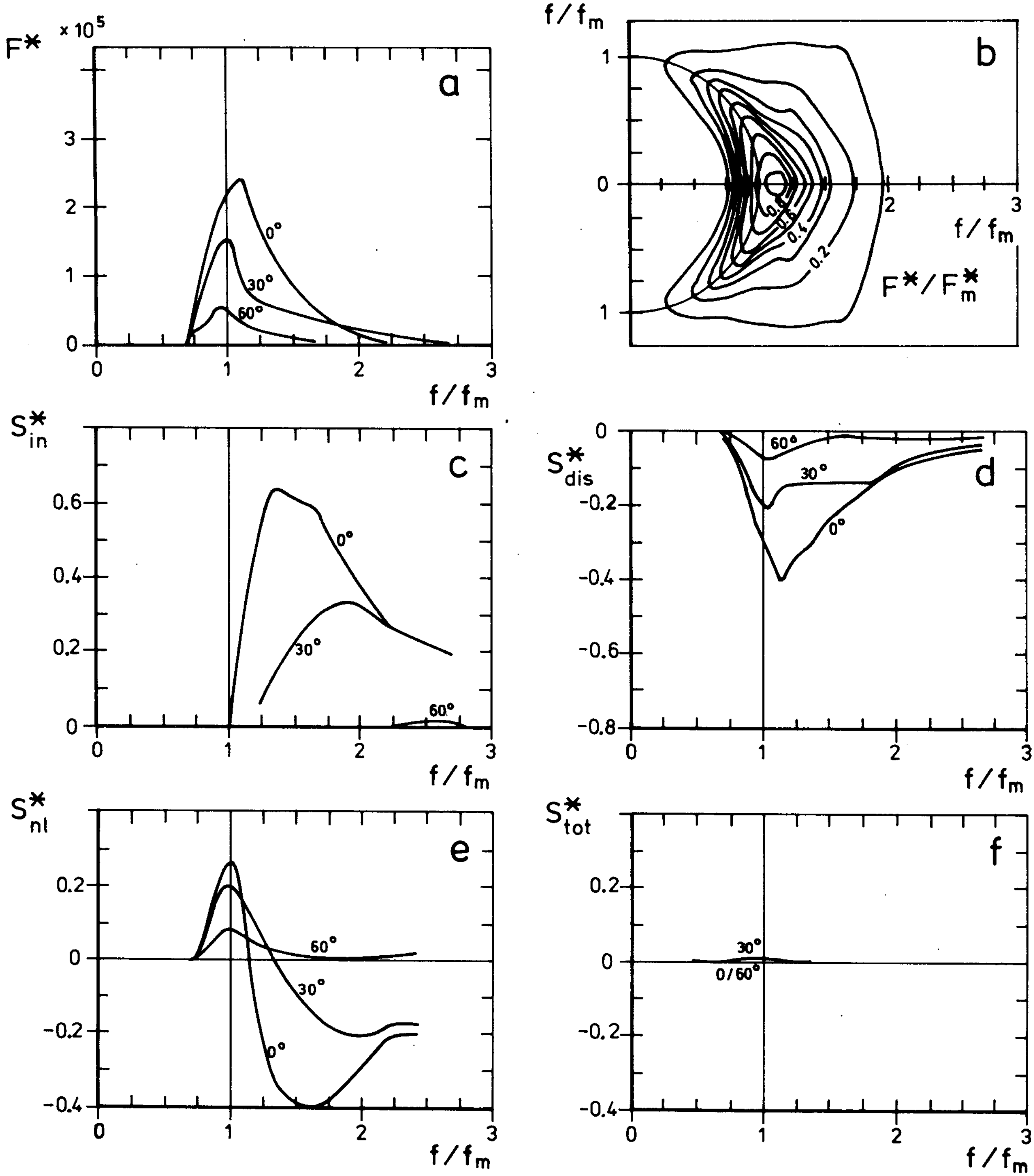

FIG. 9. Two-dimensional spectrum (panels a and b) and source function for run M2 at $x^* = 1.2 \times 10^8$. The net source function (panel f) is two orders of magnitude smaller than the individual source functions (panels c, d, e). This may be contrasted with panel f of Fig. 3, for a Pierson–Moskowitz spectrum with a prescribed spreading function. The difference may be attributed to the differences in the two-dimensional spectral distributions, cf. panels a, b, for the two cases.

the asymptotic two-dimensional spectrum that resulted from run M2 (averaged over a few successive spectra to eliminate numerical noise). The line $f/f_m = 1$ indicates the position of the peak of the corresponding one-dimensional frequency spectrum. We see immediately that our equilibrium spectrum has unusual angular properties, in that the waves in the forward direction peak at a 15% higher frequency than the one-dimensional spectrum. It is this feature that enables a nearly perfect balance between the different source terms (panel f). In the late stage of development of the spectrum the wind-input maximum is displaced to the right of the spectral peak towards higher frequencies. At the peak of the input maximum the energy transfer from the atmosphere is predominantly into waves running in the direction of the wind. This wind input into forward running waves is balanced by the energy loss due to dissipation and nonlinear transfer. The energy extracted from the waves by nonlinear interactions is transferred towards both lower and higher frequencies. A large transfer is found to occur in directions at an angle to the wind (cf. Webb, 1978; Fox, 1976; Longuet-Higgins, 1976). This explains the broadening of the spectrum at the peak energy density, to the left of the input peak. The resulting two-dimensional spectrum is very close to equilibrium, the individual source functions cancelling each other to within two orders of magnitude. The balance is clearly very delicately dependent on the precise form of the two-dimensional distribution near the peak. It would be interesting to test the predictions of this analysis by detailed directional measurements of a fully developed spectrum.

For completeness we show in Fig. 10 a comparison between the one-dimensional asymptotic spectrum and its JONSWAP fit, and in Fig. 11 the exponent $p(f)$ from a $\cos^{2p}(\theta/2)$ fit to the directional distribution of Fig. 9, together with $p(f)$ as given by Eq. (3.7).

It is of some interest to determine the relative overall contribution that each source term makes to the energy balance. For this purpose we calculated

$$\tilde{S}_i = \int_0^{2.5 f_m} S_i(f, \theta) df d\theta$$

for each source term. We obtained the ratios

$$\tilde{S}_{\rm in}:\tilde{S}_{\rm nl}:\tilde{S}_{\rm dis} = 3:(-1):(-2).$$

Since the integral of $S_{\rm nl}$ over all frequencies vanishes (the nonlinear interactions are conservative) a negative value of $\tilde{S}_{\rm nl}$ implies a transfer of energy to the high-frequency tail of the spectrum $f > 2.5 f_m$. It follows that the energy loss in the range $0 < f < 2.5 f_m$ occurs in two ways: about two-thirds of the energy is dissipated directly, while one-third is transformed to frequencies higher than $2.5 f_m$, where it is then also dissipated.

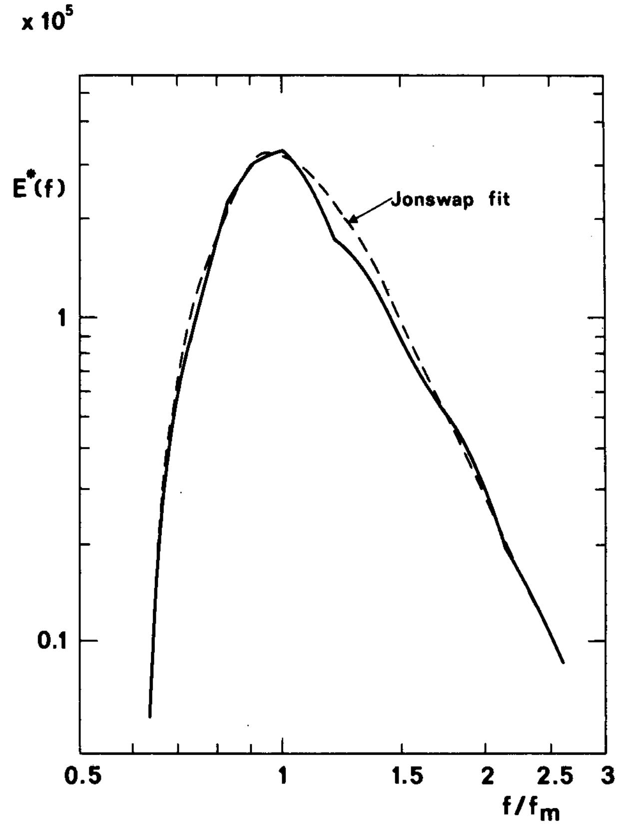

FIG. 10. JONSWAP spectral fit to the simulated spectrum for run M2 at $x^* = 1.2 \times 10^8$ (JONSWAP parameters: cf. Table 1).

5. Concluding remarks

We have shown that quasi-stationary solutions of the energy transfer equation (2.1) can exist, with source terms given by (2.4), (2.5) and (2.7), provided the dissipation parameters lie in a certain region of the parameter space.

The quasi-stationary solution M2, with a dissipation source function of the form proposed by Hasselmann (1974) for small-scale whitecapping processes, gave the closest agreement with observations and was studied in detail. The net residual of the energy balance for this case was two orders of magnitude smaller than the individual source terms. Whether this form of equilibrium actually occurs in nature cannot easily be decided, however, since it is difficult to distinguish experimentally between a small residual growth and complete stationarity. Some of the cases studied resulted in a weak asymptotic growth with frequency spectra that were also reasonably close to the Pierson–Moskowitz form. Thus a slow residual asymptotic growth cannot be excluded theoretically. (We note, however, that the distinction between no growth and weak growth at very large fetches, although

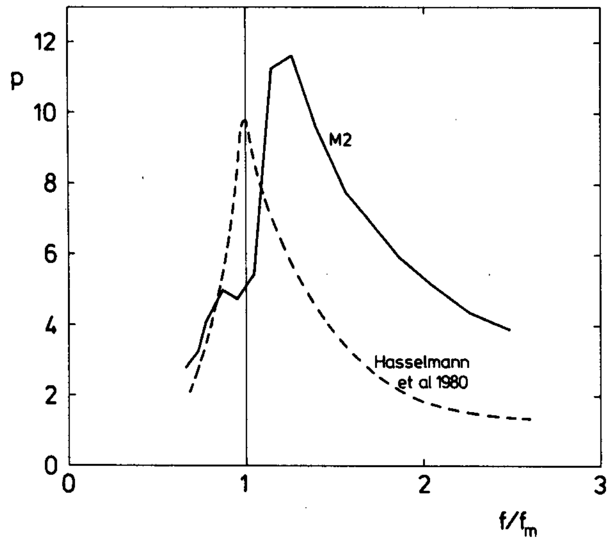

FIG. 11. Power p of spreading functions of the form (3.6) fitted to the simulated two-dimensional spectrum for run M2 at $x^* = 1.2 \times 10^8$. Also shown is the form (3.7) found by Hasselmann *et al.* (1980) for fetch limited spectra.

of theoretical interest, is not very important in practice).

The two-dimensional spectral distribution of the quasi-stationary solution M2 exhibits some interesting features. Although the one-dimensional spectrum agrees rather closely with the conventional Pierson–Moskowitz spectrum, the directional distribution does not conform to standard spreading-function assumptions. The directional distribution is narrowest at frequencies somewhat higher than the peak frequency, and is significantly broader at the peak. A number of spectral-direction measurements have indicated a minimum angular spread near the peak frequency, with a monotonically increasing spread towards both lower and higher frequencies (e.g., Mitsuyasu *et al.*, 1975; Hasselmann *et al.*, 1980; Kuik and Holthuijsen, 1981). However, the detailed fetch dependence of this feature, and the expected shift in the position of minimum spread to the right of the spectral peak in the transition stage to a fully-developed spectrum, have not been clearly established. More measurements are needed to clarify this point. Theoretically, the angular properties of the asymptotic spectrum depend, of course, on the assumed angular properties of all source terms, and future theoretical and experimental investigations should address the angular properties of both the spectrum and the source terms in more detail. However, we expect that the characteristic directional distribution found in the present study is a rather robust feature produced by the nonlinear transfer and is only weakly affected by the detailed directional properties of the other source functions.

We have investigated the spectral energy balance as originally proposed by Zakharov and Filonenko (1966) and as extended by Kitaigorodskii, 1983 (see also Kitaigorodskii *et al.,* 1975, and Zakharov and Zaslavskiy, 1982). In this approach, wind input dominates at low frequencies and the dissipation is confined to high frequencies. Energy is transformed from low to high frequencies by a constant flux through nonlinear interactions, in analogy with Kolmogorov's theory of isotropic turbulence. We find that such an energy balance, with no dissipation in the range $0 < f < 2.5f_m$ is unrealistic: it yields a spectrum which grows much too rapidly and does not approach equilibrium. The importance of direct dissipation in the energy containing range of the frequency spectrum is in agreement with a study by Bouws and Komen (1983), who analyzed an observed stationary shallow-water wind-sea spectrum. (Nevertheless, it is possible that the observed f^{-4} form of the spectrum at intermediate frequencies, cf. Kawai *et al.* (1977) and Kahma (1981), is related to the fact that the nonlinear flux divergence is indeed relatively small for this spectral form. Computations of the nonlinear transfer for other power-law spectra normally yield a too strongly pronounced minus–plus signature of the negative and high-frequency positive lobes.)

Our study of the energy balance was carried out for a single wind speed, or friction velocity. However, the analysis can be applied to arbitrary wind speeds, or friction velocities, provided the scaling laws for the input source function are known. We have chosen to scale the relevant input relation (2.4) and the relation (1.3) for the empirical fully developed Pierson–Moskowitz spectrum with the friction velocity u_*. This form of scaling follows by general dimensional arguments for any wave growth theory in which it is assumed that the structure of the atmospheric boundary layer and the interactions with the free ocean surface can be characterized by the single external parameter u_* (in addition to g). This has been proposed by Charnock (1955), Kitaigorodskii (1962) and numerous other workers, and has found increasing corroboration in recent years by field data (for neutral stability). The increase of C_{10} with wind speed according to Charnock's formula [or its approximation (2.3)] implies that the usual dimensionless Pierson–Moskowitz frequency, scaled in terms of u_{10}, decreases with increasing wind speed, while the usual dimensionless wave energy increases. Once one accepts u_*-scaling, the dependence of the drag coefficient on mean wind speed (2.3) has important consequences for wave modelling. An experimental verification of these trends would be highly desirable.

In summary, our study of the energy balance of wind-wave spectra by direct numerical integration of the transport equation based on a complete representation of all source functions supports the qualitative structure of the energy balance inferred from earlier wave growth experiments and computations of individual source functions for particular spectra. However, previous studies have suffered from inadequate knowledge of the dissipation source function. Through numerical experiments with different dissipation source functions the dependence of the asymptotic wave growth and the structure of the spectrum at large fetches on the form of dissipation could be established. A dissipation source function, Eq. (4.2), is proposed which reproduces most of the known features of a quasi-fully-developed spectrum and can be used in numerical wave models. A complementary analysis on wave growth for finite fetches, which also supports the dissipation expression (4.2), is given by Hasselmann *et al.* (1984b).

Acknowledgment. This work was supported by the Office of Naval Research under Contract N00014-77-9-0054 and the European Space Agency under Contract 5086/82. Computing facilities were made available through a special project at the European Centre for Medium Range Weather Forecasts in Reading, UK. We are grateful to ECMWF for their hospitality and the efficient support they kindly provided us.

REFERENCES

Bouws, E., and G. J. Komen, 1983: On the balance between growth and dissipation in an extreme depth-limited wind-sea in the southern North Sea. *J. Phys. Oceanogr.*, **13**, 1653–1658.

Chang, C. F., T. C. Koh, G. J. Komen and M. Subramaniam, 1983: A numerical hindcast of surface wave conditions in the South China Sea. To appear in *Proc. of 20th IAHR Conference*, Moscow.

Cartwright, D. E., 1966: Computations of the nonlinear energy transfer for a Pierson-Moskowitz spectrum. (Unpublished note.).

Charnock, H., 1955: Wind stress on a water surface. *Quart. J. Roy. Meteor. Soc.*, **81**, 639–640.

Dungey, J. C., and W. H. Hui, 1979: Nonlinear energy transfer in a narrow gravity-wave spectrum. *Proc. Roy. Soc. London*, **A368**, 239–265.

Fox, M. J. H., 1976: On the nonlinear transfer of energy in the peak of a gravity-wave spectrum II. *Proc. Roy. Soc. London*, **A348**, 467–483.

Hasselmann, D. E., M. Dunckel and J. A. Ewing, 1980: Directional wave spectra observed during JONSWAP 1973. *J. Phys. Oceanogr.*, **10**, 1264–1280.

——, J. Bösenberg, M. Dunckel, K. Richter, M. Grünewald and H. Carlson, 1984: Measurements of wave-induced pressure over surface gravity waves. *Proc. IUCRM Symp. on Wave Dynamics and Radio Probing of the Ocean Surface*, Miami, Plenum Press.

Hasselmann, K., 1960: Grundgleichungen der Seegangsvorhersage. *Schiffstechnik*, **7**, 191–195.

——, 1961: On the nonlinear energy transfer in a gravity-wave spectrum. Part 1: General theory. *J. Fluid Mech.*, **12**, 481–500.

——, 1963a: On the nonlinear energy transfer in a gravity-wave spectrum. Part 2: Conservation theorems; wave-particle analogy; irreversibility. *J. Fluid Mech.*, **15**, 273–281.

——, 1963b: On the nonlinear energy transfer in a gravity-wave spectrum. Part 3: Evaluation of the energy flux and swell-sea interaction for a Neumann spectrum. *J. Fluid Mech.*, **15**, 385–398.

——, 1974: On the spectral dissipation of ocean waves due to white capping. *Bound.-Layer Meteor.*, **6**, 107–127.

——, T. P. Barnett, E. Bouws, H. Carlson, D. E. Cartwright, K. Enke, J. A. Ewing, H. Gienapp, D. E. Hasselmann, P. Kruseman, A. Meerburg, P. Müller, D. J. Olbers, K. Richter, W. Sell and H. Walden, 1973: Measurements of wind-wave growth and swell decay during the Joint North Sea Wave Project (JONSWAP), *Dtsch. Hydrogr. Z.*, **A8**, No. 12, 95 pp.

Hasselmann, S., and K. Hasselmann, 1981: A symmetrical method of computing the nonlinear transfer in a gravity-wave spectrum. Hamburger Geophysikalische Einzelschriften, Reihe A: *Wiss. Abh.*, **52**, 163 pp.

——, and ——, 1984: The wave model Exact-NL. *Ocean Wave Modeling*, K. Hasselmann and O. M. Phillips, Eds., Vol. 2, *Proc. IUCRM Symp. on Wave Dynamics and Radio Probing of the Ocean Surface*) Miami, Plenum (In Press.)

——, K. Hasselmann, J. H. Allender and T. P. Barnett, 1984a: Improved methods of computing and parameterizing the nonlinear energy transfer in a gravity wave spectrum. (In preparation.)

——, K. Hasselmann and G. J. Komen, 1984b: Numerical experiments on fetch limited wave growth. (In preparation).

Janssen, P. A. E. M., and G. J. Komen, 1984: Effect of atmospheric stability on the growth of surface waves. *Bound.-Layer. Meteor.* (In press.)

Kahma, K. K., 1981: On the growth of wind waves in fetch-limited conditions. Report series in Geophysics, University of Helsinki, **15**, 1–93.

Kawai, S., K. Okada and Y. Toba, 1977: Support on the three-seconds power law and the $gu_*\sigma^{-4}$-spectral form for growing wind waves with field observational data. *J. Oceanogr. Soc. Japan*, **33**, 137–150.

Kitaigorodskii, S. A., 1962: Applications of the theory of similarity to the analysis of wind-generated wave motion as a stochastic process. *Izv. Akad. Nauk USSR, Geophys. Ser.*, **1**, 105–117.

——, 1983: On the theory of the equilibrium range in the spectrum of wind-generated gravity waves. *J. Phys. Oceanogr.*, **13**, 816–827.

——, V. P. Krasitskii and M. M. Zaslavskii, 1975: On Phillips' theory of equilibrium range in the spectra of wind-generated gravity waves. *J. Phys. Oceanogr.*, **5**, 410–420.

Kuik, A. J., and L. H. Holthuijsen, 1981: Buoy observation of directional wave parameters. *Proc. Conf. on Directional Wave Spectra Applications*, University of California, Berkeley, R. L. Wiegel, Ed., ASCE, 61–70.

Longuet-Higgins, M. S., 1976: On the nonlinear transfer of energy in the peak of a gravity-wave spectrum. *Proc. Roy. Soc. London*, **A347**, 311–328.

Masuda, A., 1980: Nonlinear energy transfer between wind waves. *J. Phys. Oceanogr.*, **10**, 2082–2093.

Miles, J. W., 1957: On the generation of surface waves by shear flows, Part I. *J. Fluid Mech.*, **3**, 185–204.

——, 1959: On the generation of surface waves by shear flows, Part 2. *J. Fluid Mech.*, **6**, 568–582.

Mitsuyasu, H., and T. Honda, 1982: Wind-induced growth of water waves. *J. Fluid Mech.*, **123**, 425–442.

——, F. Tasai, T. Suhara, S. Mizuno, M. Ohkuso, T. Honda and K. Rikiishi, 1975: Observations of the directional spectrum of ocean waves using a clover leaf buoy. *J. Phys. Oceanogr.*, **5**, 750–760.

Moskowitz, L., 1964: Estimates of the power spectrums for fully developed seas for wind speeds of 20 to 40 knots. *J. Geophys. Res.*, **69**, 5161–5179.

Pierson, W. J., 1964: The interpretation of wave spectrums in terms of the wind profile instead of the wind generated at a constant height. *J. Geophys. Res.*, **69**, 5191–5203.

——, and L. Moskowitz, 1964: A proposed spectral form for fully developed wind seas based on the similarity theory of S. A. Kitaigorodskii. *J. Geophys. Res.*, **69**, 5181–5190.

Plant, W. J., 1982: A relationship between wind stress and wave slope. *J. Geophys. Res.*, **87**, 1961–1967.

Regier, L. A., and R. E. Davis, 1977: Observations of the power and directional spectrum of ocean surface waves. *J. Mar. Res.*, **35**, 433–451.

Sell, W., and K. Hasselmann, 1972: Computations of nonlinear energy transfer for JONSWAP and empirical wind–wave spectra. Rep. Inst. Geophys., University of Hamburg.

Smith, S. D., 1980: Wind stress and heat flux over the ocean in gale force winds. *J. Phys. Oceanogr.*, **10**, 709–726.

——, and E. G. Banke, 1975: Variation of the sea surface drag coefficient with wind speed. *Quart. J. Roy. Meteor. Soc.*, **101**, 665–673.

Snyder, R. L., F. W. Dobson, J. A. Elliott and R. B. Long, 1981: Array measurements of atmospheric pressure fluctuations above surface gravity waves. *J. Fluid Mech.*, **102**, 1–59.

The SWAMP Group: J. H. Allender, T. P. Barnett, L. Bertotti, J. Bruinsma, V. J. Cardone, L. Cavaleri, J. Ephraums, B. Golding, A. Greenwood, J. Guddal, H. Günther, K. Hasselmann, S. Hasselmann, P. Joseph, S. Kawai, G. J. Komen, L. Lawson, H. Linné, R. B. Long, M. Lybanon, E. Maeland, W. Rosenthal, Y. Toba, T. Uji and W. J. P. de Voogt, 1984: Sea Wave Modelling Project (SWAMP). An intercomparison study of wind wave prediction models, Part 1: Principal results and conclusions. *Ocean Wave Modeling,* K. Hasselmann and O. M. Phillips, Eds; Vol. 2, *Proc. IUCRM Symp. on Wave Dynamics and Radio Probing of the Ocean Surface,* Miami, Plenum (in press).

Webb, D. J., 1978: Nonlinear transfers between sea waves. *Deep-Sea Res.*, **25**, 279–298.

Willebrand, J., 1975: Energy transport in a nonlinear and inhomogeneous random gravity wave field. *J. Fluid Mech.*, **70**, 113–126.

Wu, J., 1982: Wind-stress coefficients over sea surface from breeze to hurricane. *J. Geophys. Res.*, **87**, 9704–9706.

Zakharov, V. Ye., and N. N. Filonenko, 1966: The energy spectrum for stochastic oscillations of a fluid surface. *Dokl. Akad. Nauk SSSR,* **170,** No. 6, 1292–1295.

——, and M. M. Zaslavskiy, 1982: The kinetic equation and Kolmogorov spectra in the weak turbulence theory of wind waves. *Izv., Atmos. Oceanic Phys.*, **18,** 747–753.